MATEC Web of Conferences **96**, 00013 (2017) DOI: 10.1051/matecconf/20179600013
REE-2016

Surface Properties of Metal Hydroxide Microparticles in the Ambient Air

Valery Zakharenko[1,*], *Elena* Daibova[2], and *Natalia* Karakchieva[3]

[1]Boreskov Institute of Catalysis, Novosibirsk, Russia Federation
[2]Siberian Research Institute of Agriculture and Peat, Branch of the Siberian Federal Agrobiotechnology Research Center, Russian Academy of Sciences, Tomsk, Russia Federation
[3]Tomsk State University, Tomsk, Russian Federation

Abstract. The adsorption and photoadsorption properties of $Mg(OH)_2$ and $Ca(OH)_2$ microparticles in the ambient air were investigated. The compositional analysis of an adsorption layer of microparticles was carried out. The kinetics of photodesorption of molecules from microcrystal surfaces and the interaction of HCFC-22 (CHF_2Cl) in the dark and under light were studied. Quantum yields and their spectral dependencies were determined for CO_2 photodesorption, O_2 and CO photoadsorption. The effect of weakly bound CO displacement from the surface of microparticles was revealed during dark adsorption of HCFC-22. It is supposed that adsorbed CO is formed as a result of atmospheric CO_2 reduction after the break of Mg—OH bonds. In case of calcium hydroxide, CO is generated during the interaction of calcium hydroxide with carbon dioxide in the presence of water.

1 Introduction

From compounds containing a rare-earth element cerium, cerium dioxide CeO_2 is most widely used [1]. Introduction of cerium as addition in calcium and magnesium hydroxides substantially changes their physico-chemical properties. Before the study of these changes, it is necessary to investigate physico-chemical properties of alkaline-earth metals hydroxides.

This study is aimed at investigating of surface properties of magnesium hydroxide microparticles as well as calcium hydroxide under the conditions close to real atmosphere.

2 Experimental part

2.1 Calcium hydroxide

Industrial powdered calcium oxide ("pure" grade, "Reachem", Russia) was used as a starting compound for producing calcium hydroxide. In order to exclude in CaO the presence of calcium carbonate generated during the long-term storage of CaO, calcium oxide was heated in the air at 930 K for 4.5 hours. Due to this, calcium carbonate was decomposed into calcium oxide and carbon dioxide. The powder was cooled to room temperature (~300 K). Then a CaO suspension was prepared in distilled water and applied to the inner wall of a cylindrical quartz reactor. The surface area covered with 0.03 cm $Ca(OH)_2$ film was 70 cm^2. Calcium oxide was converted to calcium hydroxide $Ca(OH)_2$. Then water was pumped out from the reactor by a backing pump since water facilitated the conversion of calcium hydroxide to calcium carbonate in the air [2, 3]. In this way, a dense layer of calcium hydroxide without calcium carbonate impurities was supported on the reactor wall. Next, the reactor was soldered to a high-vacuum system for experiments. The reactor can be evacuated to 10^{-7} torr.

2.2 Magnesium hydroxide

For preparation of magnesium hydroxide sample, the $Mg(OH)_2$ brucite crystal has been used. The brucite crystal from the Tuva deposit was provided by the Geological Museum of the Institute of Geology and Mineralogy, Siberian Branch of the Russian Academy of Sciences, Russia. Under preparation of magnesium hydroxide sample the brucite crystal was ground in an corundum mortar in the air at room temperature. The specific surface for the obtained powder was ~ 2 m^2/g.

A suspension was prepared in distilled water from the powdered magnesium hydroxide sample by stirring and supported on the internal wall of the cylindrical quartz reactor. The reactor was similar to the reactor for $Ca(OH)_2$. Then the adsorption layer was dried in the air. The reactor with $Mg(OH)_2$ was soldered to the high-vacuum unit consisting of a gas supply system, a Pirani gauge and APDM-1 mass spectrometer (made in SU). The quantum yield of the photoadsorption (photodesorption) was found as the ratio of the quantity of photoadsorbed (photodesorbed) molecules to the number of quanta passed through the reactor's frontal (transparent) wall.

*Corresponding author: zakh@catalysis.ru

The methods for determining concentration and composition of gases in reaction mixtures, as well as the methods for calculating quantum yields and their spectral dependences are in detail described in [4, 5].

3 Results and discussion

3.1 Calcium hydroxide

In a number of conversions that occur under tropospheric conditions ($CaO \rightarrow Ca(OH)_2 \rightarrow CaCO_3$), the band gap of these compounds varies from 7.03 eV (calcium oxide) [6] to 7.3 ÷ 7.6 eV (calcium hydroxide) [7] and 5.0 eV (calcium carbonate) [8]. Due to high water vapor content (as compared to carbon dioxide), calcium oxide is converted to calcium hydroxide with the absorption spectrum shown in Fig.1 (curve 1). Its spectral dependence of absorption is close to that of calcium carbonate (Fig.1, curve 2) produced by dispersing the calcite crystal, if the absorption spectrum is registered in the shortest possible time after grinding the crystal. At the same time, if a cuvette with the powdered calcite sample is kept in the air for one month, the peak at a wavelength of 326 nm appears on the spectral dependence of absorption (Fig.1, curve 3). An inflection in spectral dependencies of absorption is recorded in calcium hydroxide (curve 1) and calcite (curve 2) in this spectral region. Any absorption in this spectral region is not observed for industrial calcium carbonate samples [9].

The study [9] supposes that the dispersion of the calcite crystal leads to the partial decomposition of calcium carbonate to CaO and CO_2. In its turn, CaO in the presence of water vapors in the air is converted to calcium hydroxide. This explains why spectral dependences of absorption of $Ca(OH)_2$ prepared in our experiment and $CaCO_3$ produced from the calcite crystal are close to each other.

After pumping out the reactor with the calcium hydroxide sample through a trap with a cool mixture (at 173 K) for a short time (~ 2 min), in reaction volume are revealed nitrogen oxides (NO and N_2O in the ratio of 1:1). These compounds are mostly desorbed from the surface of aerosol particles. It should be noted that carbon dioxide in the gas phase is not detected. The total number of molecules desorbed for a long time corresponds to 10^{17} molecules or 0.2% of the surface monolayer of the total sample in the reactor.

The mass spectrometric analysis of gases released from the surface of microcrystals showed that their primary component is nitrogen oxide (NO), with the total number of molecules in the reaction volume equal to $3 \cdot 10^{14}$ molecules.

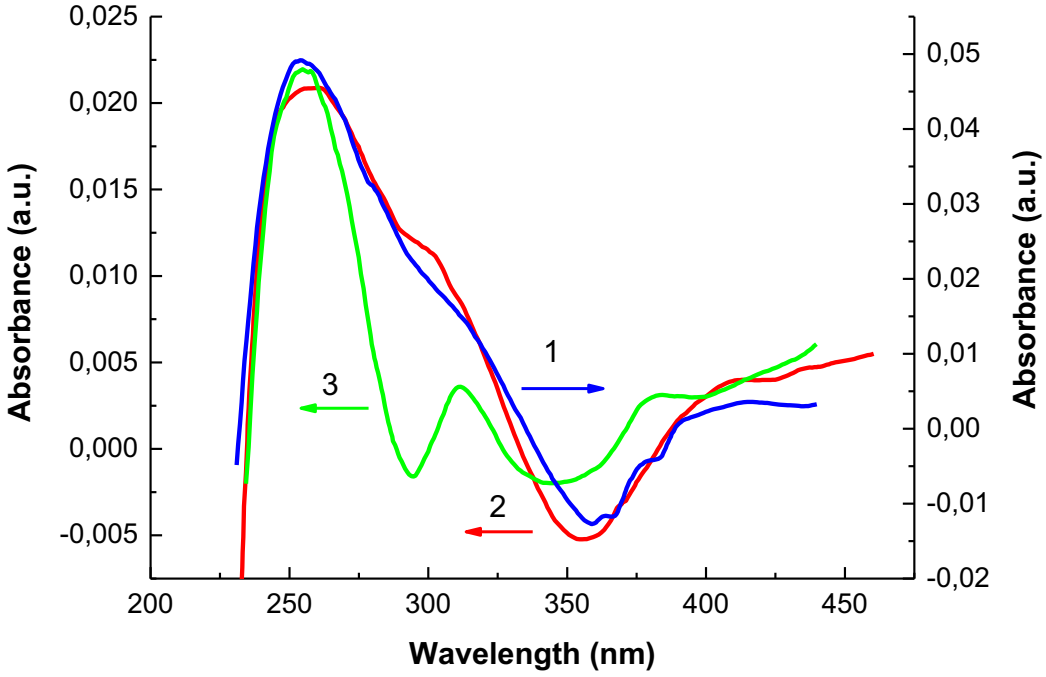

Fig. 1. Absorption spectra for the samples of calcium oxygen-containing compounds: (1) the layer of $Ca(OH)_2$ microparticles, (2) the layer of $CaCO_3$ microparticles obtained by dispersing the crystal of the mineral calcite, and (3) the second sample after one month keeping under ambient air.

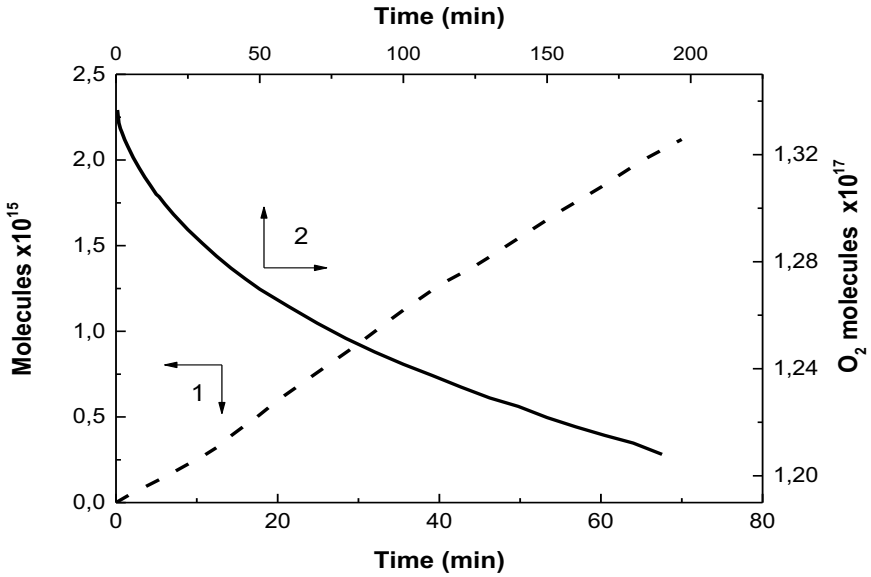

Fig. 2. Kinetics for the $Ca(OH)_2$sample: (1) photodesorption from the surface under UV filter and (2) "dark" adsorption of oxygen.

When the surface of $Ca(OH)_2$ particles is illuminated through an ultraviolet filter by the OSL-1 illuminator (made in SU) to the fullest extent, gases are photodesorbed from the sample surface. The photodesorption kinetics is shown in Fig. 2, Curve 1. According to the mass spectrometry data, nitrogen oxide NO was the primary gas in the reactor volume after photodesorption from the $Ca(OH)_2$ surface for 70 minutes.

When the NO acceptor molecule is photodesorbed, dark adsorption of the acceptor oxygen molecule takes place on adsorption centers of the surface that have been occupied by the NO acceptor molecule. The kinetics of this adsorption is shown in Fig.2, curve 2.

The numbers of adsorption centers that are occupied as a result of dark oxygen adsorption are an order of magnitude higher than the number of centers that become vacant after NO photodesorption. This indicates that oxygen adsorbed from the ambient air in the dark during the sample preparation frees surface acceptor centers, e.g., when reacting with water molecules of the reactor gas phase to produce hydrogen peroxide during the radiation of aerosol microparticles. This is confirmed by a significant increase in the seventeenth mass (OH^+) from trace amounts of hydrogen peroxide (HO-OH) in the mass spectrum as shown by the compositional analysis of gases in the reactor after photodesorption.

After dark adsorption of oxygen, the initial rate of oxygen photoadsorption was measured at a pressure of 10^{-2} torr. The rate was equal to $6 \cdot 10^{13}$ molecules·sec^{-1} when irradiated through the UV filter. For comparison, the initial photodesorption rate was 20 times lower under the same illumination conditions.

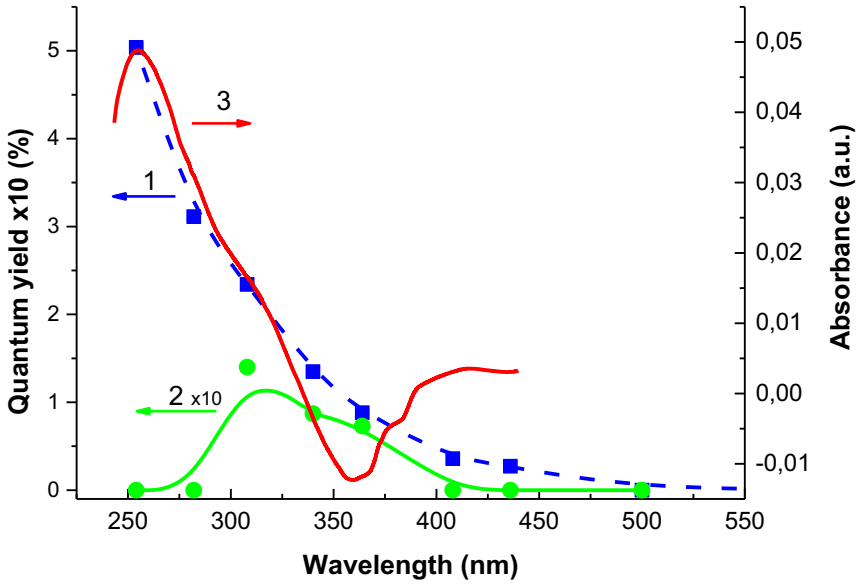

Fig. 3. Spectral dependencies for the $Ca(OH)_2$ sample: (1) quantum yield of O_2 photoadsorption, (2) quantum yield of photodesorption (scale up 10 times), and (3) absorbance relative to a reference standard (powdered MgO).

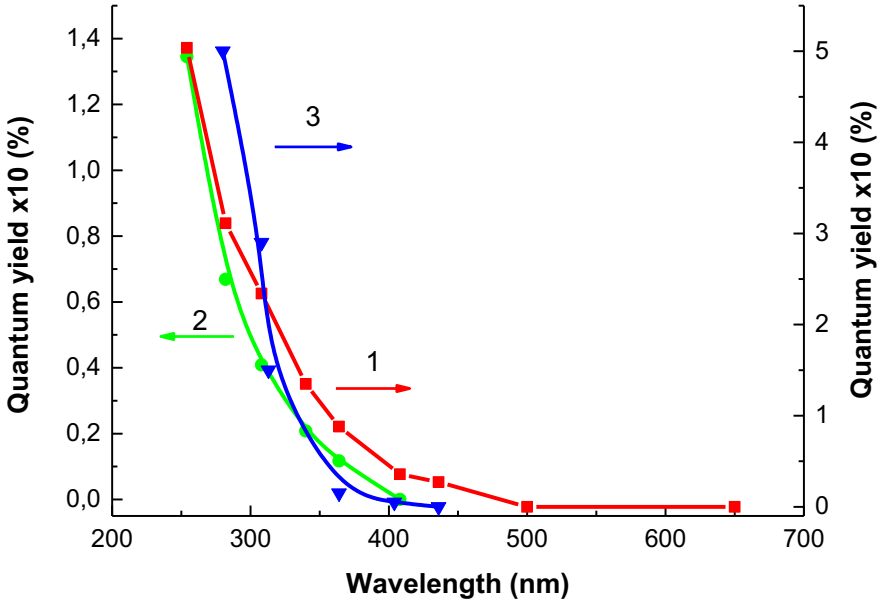

Fig. 4. Spectral dependencies of quantum yield of O_2 photosorption: (1) $Ca(OH)_2$, (2) $CaCO_3$ [9], and (3) CaO [10].

Oxygen photoadsorption and photodesorption for the calcium hydroxide sample have also different spectral dependences of quantum yields (Fig.3, curves 1 and 2 for photoadsorption and photodesorption, respectively).

Photodesorption from the surface of $Ca(OH)_2$ microparticles is observed in the spectral range from 275 nm to 400 nm (Fig. 3) with the maximum of around 300 nm, i.e. in the same spectral range as photodesorption from the surface of the sample produced by dispersing the calcite crystal ($CaCO_3$) [9].

In its turn, the spectral dependence of oxygen photoadsorption for the sample tested in this study is close to that of the calcite sample as shown in Fig.4 (curves 1 and 2 for $Ca(OH)_2$ and $CaCO_3$, respectively). Furthermore, according to [9], photoadsorption of oxygen on calcium oxide sample after its high-temperature vacuum treatment is also observed at wavelengths of shorter than 400 nm (Fig. 4, Curve 3).

According to [10], photoadsorption of oxygen in CaO occurs after absorption of a photon and electron transfer to the surface level (surface absorption of calcium oxide). Oxygen of the gas phase forms adsorbed oxygen $(O_2^-)_s$ with this electron. Both for dark oxygen adsorption in calcium oxide [11, 12] and oxygen photoadsorption in calcium oxide [10], anion vacancies of the CaO — oxygen crystal structure must be present. In this case, electron transfer from an anion vacancy that occurs as a result of photon absorption leads to the subsequent oxygen adsorption.

It can be assumed that spectral dependencies of quantum yield of oxygen photoadsorption for calcium hydroxide (Fig. 4, curve 1) and calcium carbonate (Fig.4, curve 2) are close to that for calcium oxide (Fig.4, curve 3) due to the formation of close (in terms of energy) anion vacancies in oxide, hydroxide and calcium carbonate lattices. Vacancies are generated as a result of decomposition of $Ca(OH)_2$ exposed to irradiation, as well as when the $CaCO_3$ crystal is dispersed to CaO, while CaO is reduced by radiating it in the presence of water as a reducing agent.

3.2 Magnesium hydroxide

Experiments with magnesium hydroxide samples started after degassing the reactor volume with $Mg(OH)_2$ at room temperature through a trap cooled to 173 K. CO_2, NO and CO were observed in desorption products. After 20 minutes of the accumulation, the ratio between volumes of these gases was equal to 10:0.1:1, respectively, for CO_2, NO and CO. In case of long-term accumulation of desorption products for 24 hours, the ratio changed to 20:10:1. The kinetics of carbon monoxide accumulation had a characteristic time of several minutes, while the partial pressure of desorbed CO in the gas phase reached an equilibrium value. This may indicate a weak interaction of CO with the surface of magnesium hydroxide. Slower kinetics of NO desorption (with the characteristic time of hundreds of minutes) suggest that it is formed as a result of the slowly reconstructed $Mg(OH)_2$ surface generated during the destruction of the brucite crystal in the air. Any gases (other than CO and NO) not frozen out at the liquid nitrogen temperature (77 K) were not identified in products of the gas released from the surface of magnesium hydroxide.

Desorption of nitric oxide was observed also for TiO_2 and MgO samples produced by grinding rutile and periclase crystals, respectively, in the air [4, 5].

In addition to water molecules, the surface (0001) produced from the destructed $Mg(OH)_2$ also absorbs, in the dark at room temperature, molecules of carbon dioxide and nitrous oxide contained in the air in considerable quantities [13]. The number of adsorbed molecules of these gases depends on partial pressure of the gas in the atmosphere and the adsorption capacity of

the magnesium hydroxide surface in relation to these gases.

When dispersing brucite, periclase and rutile crystals, generated surfaces of microcrystalline aerosol particles have different structures of cleavage planes {0001}, {001} and {110}, respectively, for $Mg(OH)_2$ [1], MgO [14] and TiO_2 [15]. They also differ in terms of chemical nature of surface atoms that remain after break of the respective bonds: Mg-OH for $Mg(OH)_2$, Mg-O for MgO and Ti-O for TiO_2. However, the ratio of nitrogen monoxide to carbon monoxide is similar for these three powdered samples.

Moreover, desorption of gases from the particle surface of these three aerosol samples is characterized by common features, namely:

1. carbon monoxide is weakly bound to the microparticle surface generated during the dispersion of a single crystal in the air;
2. nitrogen monoxide is slowly released from the surface as a result of its reconstruction;
3. carbon dioxide is the primary product desorbed from the surface into the gas phase.

While carbon dioxide may arise from desorption of atmospheric carbon dioxide [13], adsorbed CO and NO are likely to be result of the interaction between gas molecules of the atmosphere with the surface generated during the dispersion of the crystal in the air. For example, carbon monoxide may arise from the reduction of carbon dioxide (CO_2 content in the air is about 340 million^{-1}) by a surface metal atom with an unsaturated bond:

$$(Me\text{—})_s + CO_2 \rightarrow (CO)_s + (MeO)_s \qquad (1)$$

Nitrogen monoxide is formed by oxidation of N_2O with oxygen followed by decomposition of N_2O_2 dimer to nitrogen monoxide:

$$(O\text{—})_s + N_2O \rightarrow [Vac]_s + (N_2O_2)_s \qquad (2)$$
$$(N_2O_2)_s \rightarrow 2\,(NO)_s \qquad (3)$$

N_2O is adsorbed from the gas phase of the atmosphere during the sample preparation (0.25–0.35 million^{-1} of N_2O as a component of the uncontaminated air).

Illumination of the $Mg(OH)_2$ surface through the UV filter leads to additional desorption, mainly carbon dioxide and small amount of carbon monoxide (in the ratio of 1:10). When illuminated through the UV filter, the photodesorption rate of carbon dioxide was equal to 1.1×10^{13} molecules·sec^{-1}. The total number of photodesorbed molecules reached 1.2×10^{16} and corresponded to 0.1% of the surface monolayer of magnesium hydroxide. Photodesorption was irreversible, i.e. reverse dark adsorption did not occur after switching off the light.

After calculating the quantum yield of carbon dioxide photodesorption for different monochromatic radiation wavelengths, the spectral dependence of the quantum yield was determined. It is shown in Fig. 5 (Curve 1). The same figure shows the spectral dependence of the diffuse reflection of powdered magnesium hydroxide measured relative to magnesium oxide (Curve 2).

According to these results, the photodesorption activity of $Mg(OH)_2$ in relation to carbon dioxide is observed in the same region of the spectrum in which light absorption by the adsorbed layer of magnesium hydroxide (wavelengths less than 400 nm) is recorded.

In contrast to irreversible photodesorption of CO_2, when the $Mg(OH)_2$ surface is illuminated through the UV filter in the presence of CO, its reversible photodesorption is observed at the initial rate of 4.2×10^{13} molecules · sec $^{-1}$. The amount of photoadsorbed CO reached 7.1×10^{13} molecules · sec $^{-1}$. After turning off the light, the photoadsorbed CO is completely released into the gas phase.

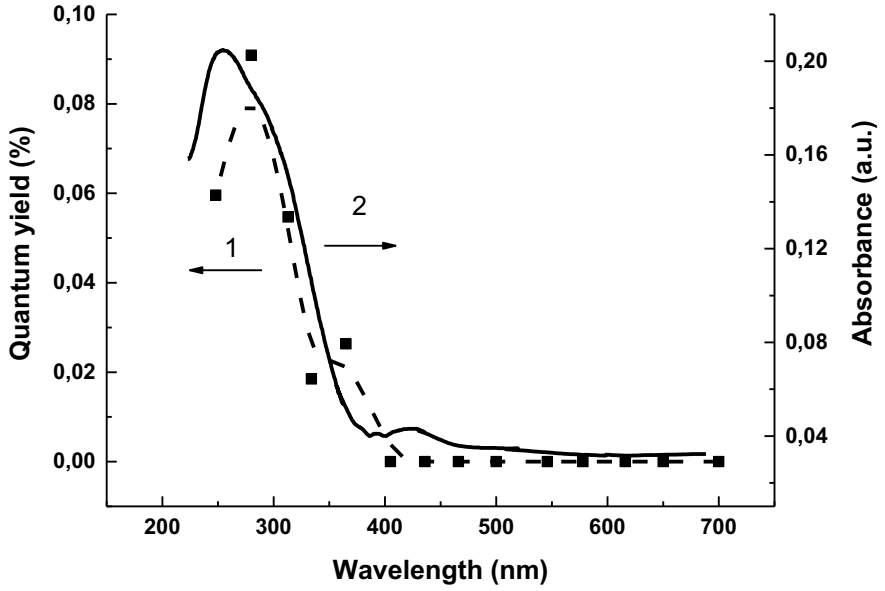

Fig. 5. Spectral dependencies for the $Mg(OH)_2$ sample: (1) quantum yield of CO_2 photodesorption on the microparticles obtained by dispersing the crystal of the mineral brucite and (2) absorbance relative to a reference standard (powdered MgO).

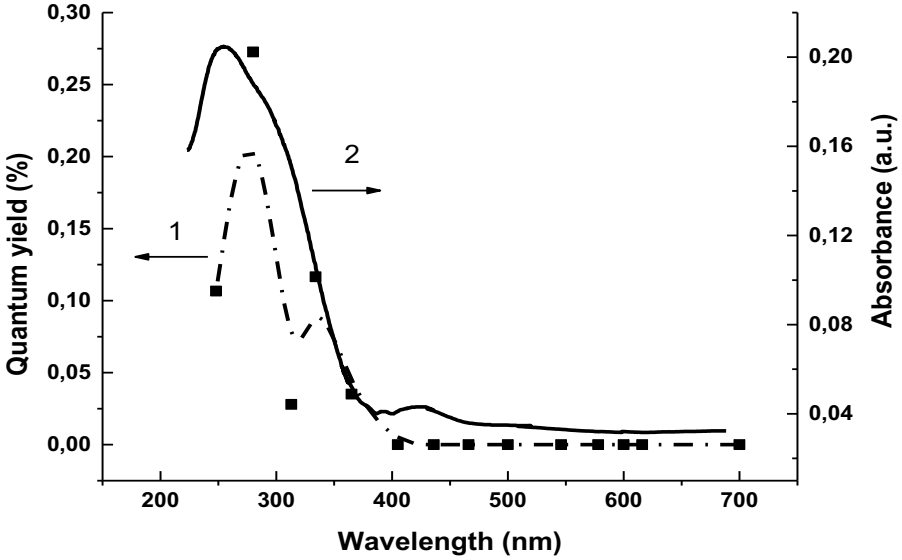

Fig. 6. Spectral dependencies for the $Mg(OH)_2$ sample: (1) quantum yield of CO photoadsorption on the microparticles obtained by dispersing the crystal of the mineral brucite and (2) absorbance relative to a reference standard (powdered MgO).

The spectral dependence of the quantum yield of CO photoadsorption (Fig. 6, Curve 1) is close to the spectral dependence of CO_2 photodesorption (Fig. 5, Curve 1) and to the spectrum of absorption by the adsorbed layer of magnesium hydroxide (Fig. 6, Curve 2).

Thus, the absorption of photons from a wavelength region of less than 400 nm leads to both photodesorption of CO_2 and photoadsorption of CO; however, the formation of CO_2 on the magnesium hydroxide surface is not associated with CO photoadsorption. The following mechanism of photoprocesses can be proposed:

$$\text{V.B.} + [\text{Vac}]_s \xrightarrow{h\nu} h_{v.b.} + [e]_s \quad (4)$$

$$(CO_2^-)_s + h_{v.b.} \rightarrow CO_2 \quad (5)$$

$$CO + [e]_s \rightarrow CO{-}[e]_s \quad (6)$$

where **V.B.** is the valence band of magnesium hydroxide, $\mathbf{[Vac]_s}$ is the surface vacancy, $\mathbf{h_{v.b.}}$ is the "free" hole in the valence band, $\mathbf{[e]_s}$ is the electron in the valence band, $\mathbf{CO{-}[e]_s}$ is the weakly bound carbon monoxide.

3.3 Interaction of HCFC-22 with the $Mg(OH)_2$ and $Ca(OH)_2$ microparticle surfaces

During the adsorption of HCFC-22, its dark adsorption rate exceeds the rate of simultaneous CO desorption from the $Mg(OH)_2$ surface. While in case of industrial MgO, the dark adsorption rate of HCFC-22 is 4 times less than the rate of simultaneous CO desorption [16], in case of $Mg(OH)_2$ the adsorption rate of HCFC-22 is two times higher than the CO desorption rate.

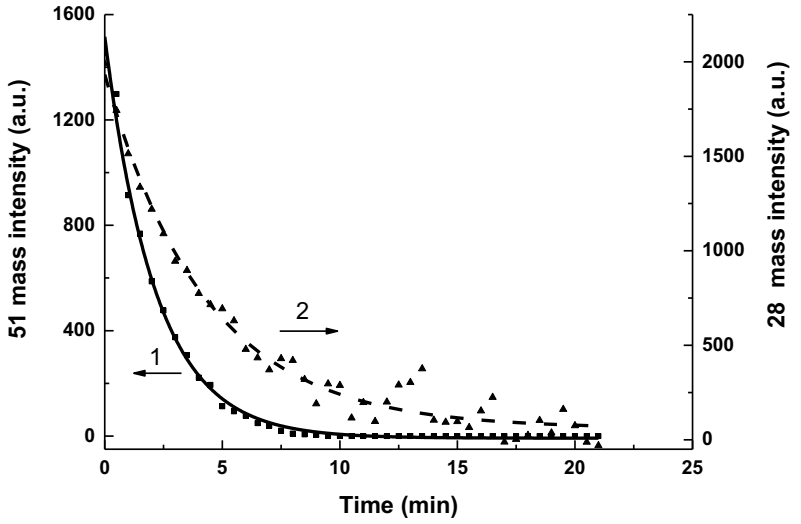

Fig. 7. Kinetics for the $Mg(OH)_2$ sample: (1) "dark" adsorption of Freon 22 (51 mass intensity) and (2) decreasing the adsorbed CO amount from the surface (28 mass intensity).

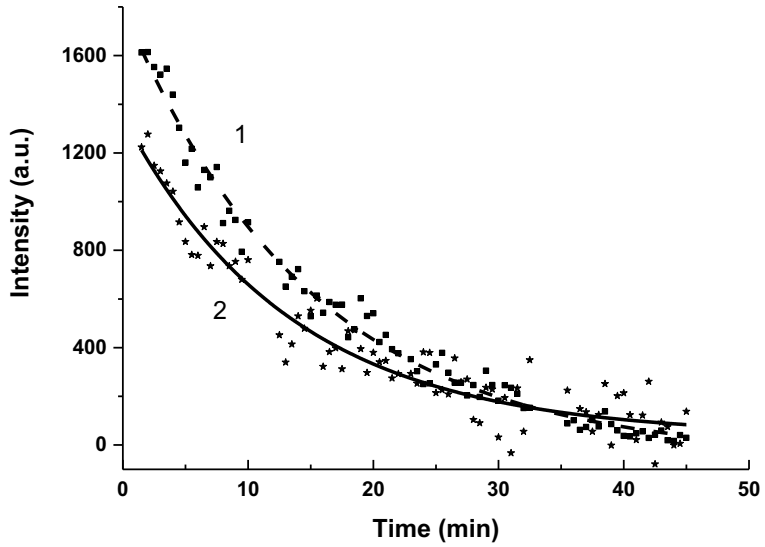

Fig. 8. Kinetics for the $Ca(OH)_2$ sample: (1) "dark" adsorption of Freon 22 (51mass intensity) and (2) decreasing the adsorbed CO amount from the surface (28 mass intensity).

According to the mass spectrometry data for the second supply of HCFC-22, both its adsorption kinetics and CO desorption kinetics are approximated by first-order equations (Fig. 7, Curves 1 and 2, respectively, for HCFC-22 and CO). With an increasing amount of HCFC-22 adsorbed in the dark, its adsorption rate decreases after pumping out produced carbon monoxide and supplying a "new" portion of HCFC-22.

At the first supply of HCFC-22, the dark adsorption rate of HCFC-22 on the surface of a part of calcium hydroxide is close to the rate of carbon dioxide release from the $Ca(OH)_2$ surface. Further, when carbon monoxide is pumped out and a "new" portion of HCFC-22 is supplied, the dark adsorption rate of HCFC-22 decreases but still exceeds the CO desorption rate (Fig. 8).

Thus, adsorption of HCFC-22 displaces the weakly adsorbed carbon monoxide, a part of which is desorbed when $Mg(OH)_2$ and $Ca(OH)_2$ samples are pumped out. Magnesium hydroxide is known to have high adsorption capacity relative to chlorine compounds and is used as a component of mixtures for removing such compounds from gases [17]. The high adsorption capacity of magnesium and calcium hydroxides is indicated by a high degree of filling $Mg(OH)_2$ and $Ca(OH)_2$ microparticle surfaces observed in this study: it exceeds 10% of their surface monolayer.

In our opinion, the formation of weakly bound carbon dioxide on the surface of MgO and $Mg(OH)_2$ produced by dispersing MgO periclase and $Mg(OH)_2$ brucite crystals is associated with broken Mg – O [5] and Mg – OH bonds (Equation 1) and the reduction of adsorbed carbon dioxide to carbon oxide. However, the calcium hydroxide sample was not produced from the $Ca(OH)_2$ portlandite crystal. In this case, it can be assumed that the formation of carbon oxide in the reaction volume of adsorbed water and water in gas phase takes place during the interaction between $Ca(OH)_2$ and carbonic acid, e.g., through the reaction:

$$Ca(OH)_2 + H_2CO_3 \rightarrow CO + H_2O_2 + CaO + H_2O \quad (7)$$

After having been saturated with HCFC-22, surfaces of magnesium and calcium hydroxides samples were exposed to light through the UV filter which transmitted radiation with wavelengths of 235 to 410 nm. The mass spectrometry data show that, when exposed to such light, photoadsorption of HCFC-22 and, at the same time, photodesorption of carbon monoxide are observed. Using the Pirani gauge, we recorded a decrease in the total pressure at the rate of ~ 10^{12} molecules · sec^{-1}.

Thus, the surface of $Mg(OH)_2$ and $Ca(OH)_2$ aerosol microparticles exposed to light in the presence of HCFC-22 results in a slight increase in its adsorption rate as compared to dark adsorption of HCFC-22.

4 Conclusions

Thus, the study of calcium hydroxide without calcium carbonate impurities demonstrates that there is no carbon dioxide on the surface of the calcium hydroxide aerosol microparticles. The photochemical activity in relation to oxygen photoadsorption and photodesorption of gases from the surface of aerosol particles is observed at the wavelengths of photons shorter than 400 nm. Photoadsorption of oxygen in oxygen-containing compounds of CaO, $Ca(OH)_2$ and $CaCO_3$ have similar mechanisms associated with the formation of anion vacancies in the lattice structure of these compounds.

The effect of weakly bound CO displacement from the surface of magnesium and calcium microparticles was revealed during the dark adsorption of HCFC-22. It is supposed that carbon monoxide is formed as a result of atmospheric CO_2 reduction after breaking Mg—OH bonds during the dispersion of the brucite crystal in the air. The formation of carbon oxide on the calcium hydroxide surface in the reaction volume of adsorbed

water and water in gas phase takes place during the interaction between $Ca(OH)_2$ and carbonic acid.

This work was conducted within the framework of budget project No. 0303-2016-0002 for Boreskov Institute of Catalysis.

References

1. K. Reinhardt and H. Winkler in "Cerium Mischmetal, Cerium Alloys, and Cerium Compounds" in *Ullmann's Encyclopedia of Industrial Chemistry* (Wiley-VCH, Weinheim, 2000)
2. Ch. Theocharis, D. Yeates, Colloids and Surface, **58**, 353 (1991)
3. G. Montes-Hernandez, A. Pommerol, F. Renard, P. Beck, E. Quirico, O. Brissaud, J. Chem. Eng., **161**, 250 (2010)
4. V.S. Zakharenko and E.B. Daibova, Atmos. Ocean Optics, **22**, 611 (2009)
5. V.S. Zakharenko and E.B. Daibova, Atmos. Ocean Optics, **24**, 516 (2009)
6. R.C. White, W.C.Walker, Phys. Rev. Lett., **22**, 1428 (1969)
7. A. Pishtshev, S.Zh. Karazhanov, M. Klepov, Computation Mater. Sci., **95**, 693 (2014)
8. M.G. Brik, Physica B: Condensed Matter., **406**, 1004 (2011)
9. V.S. Zakharenko and E.B. Daibova, Atmos. Ocean Optics, **28**, 540 (2015)
10. A.M. Volodin, V.A. Bolshov, T.A. Konovalova, Molecular Eng.,**4**, 221 (1994)
11. D. Cordishi, V. Indovina, M.Occhiuzzi, J. Chem. Soc. Faraday Trans. I, **74**, 883 (1978)
12. M. Che, S. Coluccia, A.Zecchina, J. Chem. Soc. Faraday Trans. I, **74**, 1324 (1978)
13. P. Brimblecombe, *Air Composition and Chemistry* (Academic Press, New York, 1988)
14. S. Benedetti, P. Torelli, P. Luches, E. Gualtieri, A. Rota, S. Valeri, Surf. Sci., **601**, 2636 (2007)
15. W.S. Epling, Ch.H.F. Pedan, M.A. Henderson, U. Diebold, Surf. Sci., **412/413**, 333 (1998)
16. V.S. Zakharenko and V.N. Parmon, Kinet. I Katal., **41**, 834 (2000)
17. X.-F. Wu, G.-H. Hu, B.-B. Wang, Y.-F. Yang, J. Crystal Growth., **310**, 457 (2008)